Available online at www.sciencedirect.com
ScienceDirect
Journal of Fluorine Chemistry 128 (2007) 139–143
JOURNAL OF FLUORINE CHEMISTRY
www.elsevier.com/locate/fluor

Synthesis of $LiNi_{1/3}Co_{1/3}Mn_{1/3}O_{2-z}F_z$ cathode material from oxalate precursors for lithium ion battery

Yu-Shi He, Li Pei, Xiao-Zhen Liao, Zi-Feng Ma *

Department of Chemical Engineering, Shanghai Jiao Tong University, Shanghai 200240, PR China

Received 2 October 2006; received in revised form 25 October 2006; accepted 4 November 2006
Available online 9 November 2006

Abstract

The layered $LiNi_{1/3}Co_{1/3}Mn_{1/3}O_{2-z}F_z$ ($0 \leq z \leq 0.12$) cathode materials were synthesized from oxalate precursors by a simple self-propagating solid-state metathesis method with the help of the ball milling and the following calcination. $Li(Ac)\cdot 2H_2O$, $Ni(Ac)_2\cdot 4H_2O$, $Co(Ac)_2\cdot 4H_2O$, $Mn(Ac)_2\cdot 4H_2O$(Ac = acetate), LiF and excess $H_2C_2O_4\cdot 2H_2O$ were used as starting materials without any solvent. The structural and electrochemical properties of the prepared $LiNi_{1/3}Co_{1/3}Mn_{1/3}O_{2-z}F_z$ were characterized by X-ray diffraction (XRD), field emission scanning electron microscopy (FESEM) and electrochemical measurements, respectively. The XRD patterns indicate that all samples have a typical hexagonal structure with a space group of $R\bar{3}m$. The FESEM images show that the primary particle size of $LiNi_{1/3}Co_{1/3}Mn_{1/3}O_{2-z}F_z$ gradually increases with increasing fluorine content. Though the fluorine-substituted $LiNi_{1/3}Co_{1/3}Mn_{1/3}O_{2-z}F_z$ have lower initial discharge capacities, a small amount of fluorine-substituted $LiNi_{1/3}Co_{1/3}Mn_{1/3}O_{2-z}F_z$ ($z = 0.04$ and 0.08) exhibit excellent cycling stability and rate capability compared to fluorine-free $LiNi_{1/3}Co_{1/3}Mn_{1/3}O_2$.

Keywords: Lithium-ion battery; Self-propagating solid-state metathesis method; $LiNi_{1/3}Co_{1/3}Mn_{1/3}O_2$; Fluorine substitution; Rate capability

1. Introduction

Recently, layer-structured $LiNi_{1/3}Co_{1/3}Mn_{1/3}O_2$ compound developed by Ohzuku and Makimura [1] has been considered as a promising candidate of next-generation cathode materials to replace $LiCoO_2$ for rechargeable lithium ion batteries due to its large capacity and stable structure. The structure stability and cycling performance of $LiNi_{1/3}Co_{1/3}Mn_{1/3}O_2$ could be improved by doping or substituting various ions such as Mg [2], Mo [3], Al [4], Fe [4,5], Si [6], Cr [7], and F [8,9]. It was reported that the fluorine substitution for oxygen into spinel-structured or layer-structured cathode materials was effective for the improvement of electrochemical performance due to fluorine's ability to stabilize metastable structures [8–14]. Amatucci et al. [12] reported that the fluorine substitution could improve cycling performance of spinel $LiAl_xMn_{2-x}O_4$ at high temperature (55 °C). Wu et al. [13] pointed out that F–Al-substituted spinel could suppress the Jahn-Teller instability to improve the cycling performance better than $LiMn_2O_4$. Kang and Amine [14] reported that F-substituted $Li(Li_{0.2}Ni_{0.15+0.5z}Co_{0.10}Mn_{0.55-0.5z})O_{2-z}F_z$ exhibited better cycling performance whether at room temperature or high temperature (55 °C) than non-substituted material and the impedance was also significantly reduced by the fluorine substitution. Various preparation methods have been reported for $LiNi_xCo_yMn_{1-x-y}O_2$, such as co-precipitation [15–19] method, sol–gel method [20], and glycine-nitrate combustion method [21]. The traditional co-precipitation method could give phase-pure oxide products and high tap-density spherical powders with uniform distribution. But the co-precipitation method has rather complicated processes such as washing, filtering, and precalcination. Thus, it is very difficult to reproductively prepare the same sample. So, it is necessary to develop a new synthesis route for $LiNi_xCo_yMn_{1-x-y}O_2$ compound. Caballero et al. [22] developed a simple solvent-free method for preparing nanometric cathode materials, including $LiMn_2O_4$, $LiNi_{0.5}Mn_{1.5}O_4$, $LiCoO_2$ and $LiCo_{0.5}Ni_{0.5}O_2$. The method is based on the preparation of oxalate precursor by one-step

* Corresponding author. Tel.: +86 21 54742894; fax: +86 21 54741297.
E-mail address: zfma@sjtu.edu.cn (Z.-F. Ma).

0022-1139/$ – see front matter © 2006 Elsevier B.V. All rights reserved.
doi:10.1016/j.jfluchem.2006.11.002

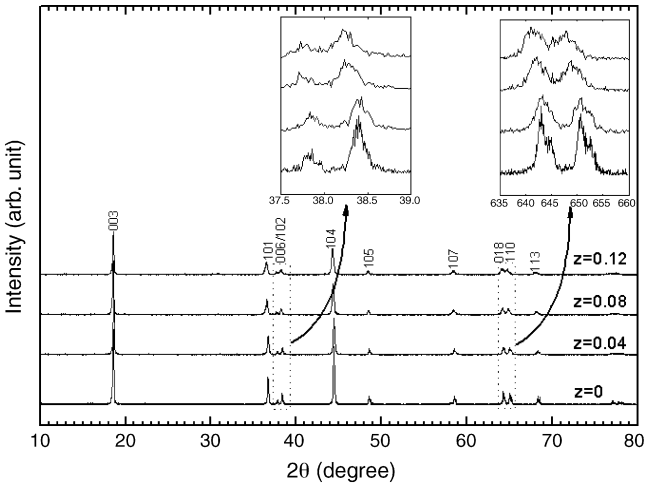

Fig. 1. X-ray diffraction patterns of $LiNi_{1/3}Co_{1/3}Mn_{1/3}O_{2-z}F_z$ samples with different fluorine contents.

solid-state metathesis reactions of various hydrated salts in the presence of hydrated oxalic acid [23,24]. In the solid-state metathesis procedure, no solvent is added which could effectively avoid the occurrence of concentration gradient in precursor and simplify the preparation process. Furthermore, this method could ensure uniform distribution of doped ions in the precursor due to the contribution of the solid-state metathesis reactions. In this paper, the phase-pure $LiNi_{1/3}Co_{1/3}Mn_{1/3}O_{2-z}F_z$ ($z = 0$, 0.04, 0.08 and 0.12) were synthesized by self-propagating solid-state metathesis method from oxalate precursors. The effects of fluorine substitution on the structure, morphology and electrochemical properties of the $LiNi_{1/3}Co_{1/3}Mn_{1/3}O_{2-z}F_z$ cathode materials were also investigated.

2. Results and discussion

Fig. 1 shows the XRD patterns of $LiNi_{1/3}Co_{1/3}Mn_{1/3}O_{2-z}F_z$ materials with various fluorine contents obtained by calcining the oxalate precursors at 900 °C for 20 h in air atmosphere. The XRD patterns of all samples could be indexed by a hexagonal α-$NaFeO_2$ structure (space group: 166, $R\bar{3}m$) and no obvious impurity phase peaks could be observed, indicating that the synthesized samples were single phase. In XRD patterns, the integrated intensity ratio of (0 0 3)/(1 0 4) peak and the spliting of (0 0 6)/(1 0 2) peak and (0 1 8)/(1 1 0) peak are regarded as the indications of characteristic of layered structure materials [25]. It was reported that the undesirable cation mixing would take place if the integrated intensity ratio of (0 0 3)/(1 0 4) peak is less than 1.2. According to the insets illustrated in Fig. 1, the (0 0 6) and (1 0 2) peaks and (0 1 8) and (1 1 0) peaks are clearly split in all the XRD patterns, which means the formation of well hexagonal layered ordering structure. The integrated intensity ratio of (0 0 3)/(1 0 4) peaks and the lattice parameters calculated by the least-square method using ten diffraction lines from XRD data are listed in Table 1. With the increase of fluorine content, the integrated intensity ratio of (0 0 3)/(1 0 4) peak declines from 1.26 ($z = 0$) to 0.92 ($z = 0.08$) indicating that the degree of cation mixing increases. The lattice parameter a corresponds to become large with increasing fluorine content, which could be attributed to larger Co^{2+} (0.65 Å) than Co^{3+} (0.545 Å) [8]. When fluorine contents are morn than 0.08, the decrease of lattice parameter c may be because the effect of the replacement of O^{2-} (1.40 Å) by smaller F^- (1.33 Å) exceeds the effect of the increase of the radii of reduced transition metal ions.

The field-emission SEM (FESEM) images of $LiNi_{1/3}Co_{1/3}Mn_{1/3}O_{2-z}F_z$ ($z = 0$, 0.04, 0.08 and 0.12) materials are shown in Fig. 2. The fluorine-free $LiNi_{1/3}Co_{1/3}Mn_{1/3}O_2$ has a relative uniform particle distribution ranging from 100 to 250 nm. With increasing fluorine content, the primary particle size gradually increases and the shape of the primary particles obviously changes. The similar morphological change with fluorine substitution was previously reported [26]. Furthermore, the grains agglomerate much more closely as the fluorine content increases, which is useful to the improvement of tap density.

Fig. 3 shows the typical initial charge-discharge curves of $LiNi_{1/3}Co_{1/3}Mn_{1/3}O_{2-z}F_z$ ($z = 0$, 0.04, 0.08 and 0.12) materials. The cycling performance for the prepared $LiNi_{1/3}Co_{1/3}Mn_{1/3}O_{2-z}F_z$ materials is illustrated in Fig. 4. The cell was cycled between 3 and 4.6 V at a charge/discharge current density of 32 mA g^{-1} (0.2 C) at room temperature. As shown in Fig. 3, all the cells display stable and smooth charge/discharge curves without any plateaus. This indicates that no spinel-related phases are formed during charging and discharging [27]. The first discharge capacities of $LiNi_{1/3}Co_{1/3}Mn_{1/3}O_{2-z}F_z$ are 199 mAh g^{-1} ($z = 0$), 177 mAh g^{-1} ($z = 0.04$), 169 mAh g^{-1} ($z = 0.08$) and 135 mAh g^{-1} ($z = 0.12$), respectively. The initial discharge capacities decrease with increasing the substitution amount of fluorine. Moreover, the fluorine-substituted materials exhibit higher charge voltages. It could be considered that the existence of the strong bond of Li–F in $LiNi_{1/3}Co_{1/3}Mn_{1/3}O_{2-z}F_z$ would disturb intercalation of Li^+ ions, which leads to the decrease of initial discharge capacity and the increase of charge voltage [28]. According to Fig. 4, the fluorine-free $LiNi_{1/3}Co_{1/3}Mn_{1/3}O_2$ delivers a highest initial discharge capacity. However, the retention value of capacity is only 83.5% after 30 cycles.

Table 1
Lattice parameters and structure parameters of $LiNi_{1/3}Co_{1/3}Mn_{1/3}O_{2-z}F_z$ ($z = 0$, 0.04, 0.08 and 0.12) samples calcined at 900 °C for 20 h

Samples	Compounds	a (Å)	c (Å)	Volume (Å^3)	c/a	$I_{(0\,0\,3)}/I_{(1\,0\,4)}$[a]
1	$LiNi_{1/3}Co_{1/3}Mn_{1/3}O_2$	2.865	14.261	101.35	4.978	1.26
2	$LiNi_{1/3}Co_{1/3}Mn_{1/3}O_{1.96}F_{0.04}$	2.868	14.273	101.51	4.977	1.19
3	$LiNi_{1/3}Co_{1/3}Mn_{1/3}O_{1.92}F_{0.08}$	2.872	14.292	102.12	4.976	1.17
4	$LiNi_{1/3}Co_{1/3}Mn_{1/3}O_{1.88}F_{0.12}$	2.879	14.287	102.58	4.962	0.92

[a] $I_{(0\,0\,3)}/I_{(1\,0\,4)}$ is the ratio of the integrated intensities of the (0 0 3) and (1 0 4) peaks.

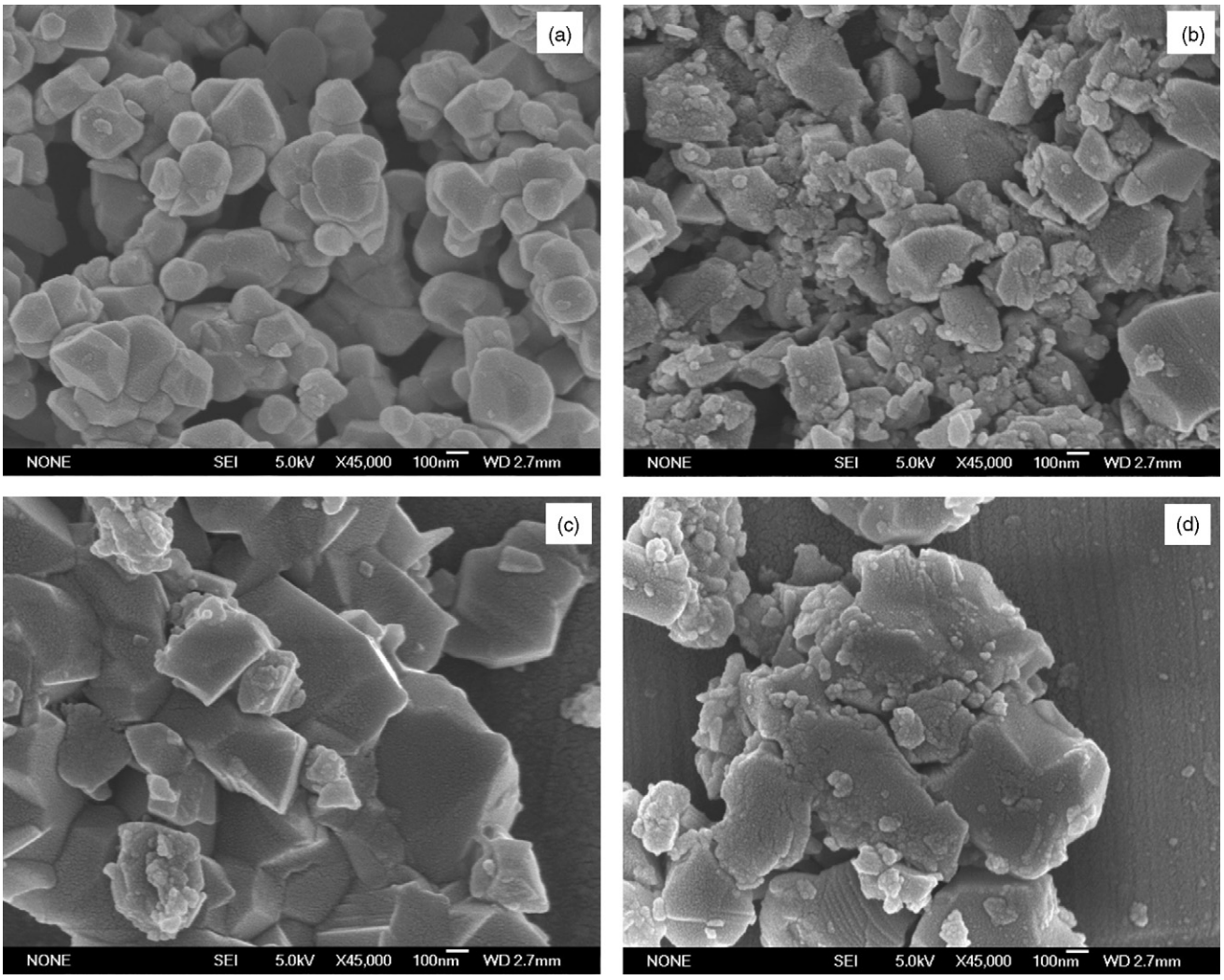

Fig. 2. FESEM images of $LiNi_{1/3}Co_{1/3}Mn_{1/3}O_{2-z}F_z$ ($0 \leq z \leq 0.12$) samples (a) $z = 0$; (b) $z = 0.04$; (c) $z = 0.08$; and (d) $z = 0.12$.

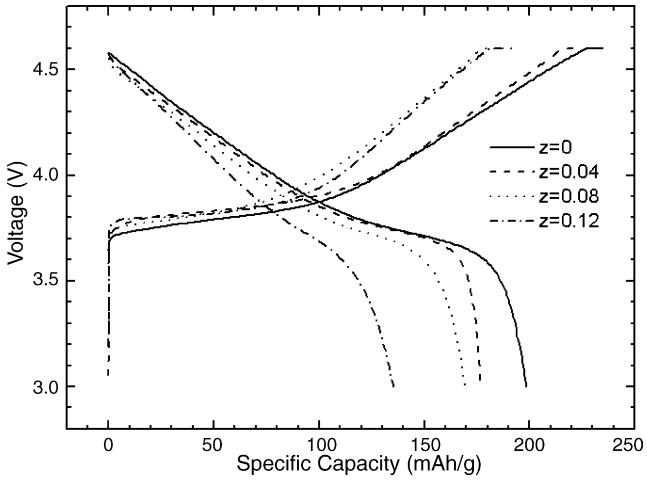

Fig. 3. Initial charge-discharge curves of $LiNi_{1/3}Co_{1/3}Mn_{1/3}O_{2-z}F_z$ samples in the voltage range 3–4.6 V at a charge/discharge current density of 32 mA g^{-1} (0.2 C) at room temperature.

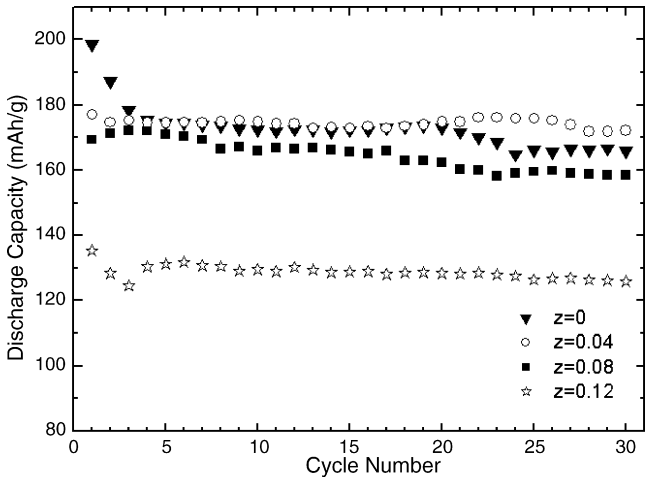

Fig. 4. Cycling performance of $LiNi_{1/3}Co_{1/3}Mn_{1/3}O_{2-z}F_z$ samples between 3 and 4.6 V at 0.2 C rate at room temperature.

Although the fluorine-substituted materials have lower initial discharge capacities, they show excellent cycling stability and better capacity retentions. The capacity retentions could still attain 97.3% for $z = 0.04$, 93.4% for $z = 0.08$ and 93.0% for $z = 0.12$ after 30 cycles, respectively. Moreover, the discharge capacity of $LiNi_{1/3}Co_{1/3}Mn_{1/3}O_{1.96}F_{0.04}$ is higher than that of the fluorine-free material after 5 cycles. The excellent cycling performance of fluorine-substituted materials might be due to the existence of the strong bond by Li-F in the host structure which could protect the active material from HF attack in the electrolyte, especially at high upper cutoff voltage operation [2]. It is obvious that the existence of a small amount of fluorine could significantly improve the cycling performance of $LiNi_{1/3}Co_{1/3}Mn_{1/3}O_{2-z}F_z$ and doesn't obviously affect the discharge capacity of the samples.

The effect of fluorine substitution on the rate capability between 3 and 4.6 V is showed in Fig. 5. The $Li/LiNi_{1/3}Co_{1/3}Mn_{1/3}O_{2-z}F_z$ ($z = 0$, 0.04, 0.08 and 0.12) cells were charged using a constant current density of 32 mA g^{-1} (0.2 C) before each discharge and discharged under the constant currents of 32 mA g^{-1} (0.2 C), 80 mA g^{-1} (0.5 C), 160 mA g^{-1} (1 C), 320 mA g^{-1} (2 C), 800 mA g^{-1} (5 C), 1600 mA g^{-1} (10 C), 2400 mA g^{-1} (15 C), 3200 mA g^{-1} (20 C), respectively. The fluorine-free $LiNi_{1/3}Co_{1/3}Mn_{1/3}O_2$ displays the highest discharge capacity at low C-rates. However, $LiNi_{1/3}Co_{1/3}Mn_{1/3}O_{1.96}F_{0.04}$ and $LiNi_{1/3}Co_{1/3}Mn_{1/3}O_{1.92}F_{0.08}$ show better rate capability and capacity retention than the fluorine-free material above 0.5 C rate. $LiNi_{1/3}Co_{1/3}Mn_{1/3}O_{1.92}F_{0.08}$ presents a capacity of 128 mAh g^{-1} at 5 C rate, corresponding to 76.3% capacity retention compared to its capacity at 0.2 C. As the rate rises to 20 C, the discharge capacity of $LiNi_{1/3}Co_{1/3}Mn_{1/3}O_{1.92}F_{0.08}$ could still reach 55 mAh g^{-1}, showing 32.9% capacity retention. The good rate capability of fluorine-substituted materials could be attributed to the existence of the strong bonding by F which stabilizes the host structure and increases the stability of cathode material against HF attack [26]. These results indicate that fluorine substitution is an effective method to noticeably enhance the rate capability of $LiNi_{1/3}Co_{1/3}Mn_{1/3}O_2$.

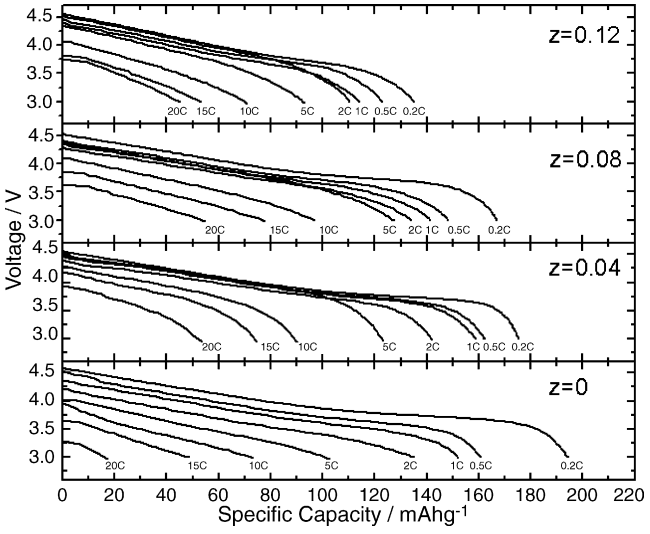

Fig. 5. Rate capability tests for $LiNi_{1/3}Co_{1/3}Mn_{1/3}O_{2-z}F_z$ samples in voltages of 3–4.6 V at room temperature.

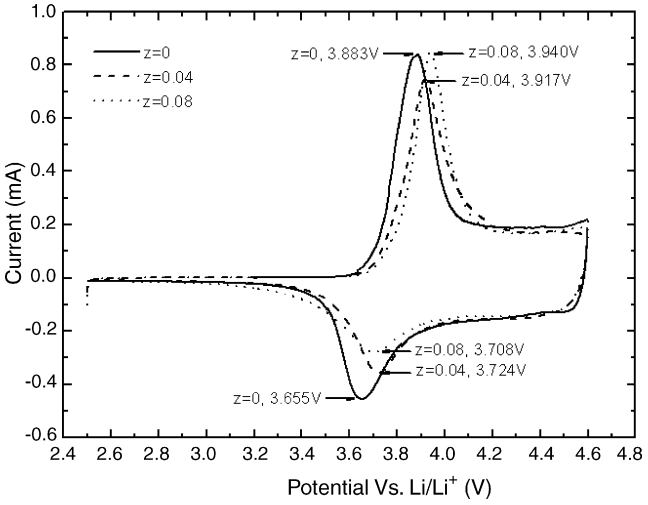

Fig. 6. CVs of $LiNi_{1/3}Co_{1/3}Mn_{1/3}O_{2-z}F_z$ ($z = 0$, 0.04 and 0.08) cathode material in an electrolyte of 1 M $LiPF_6$ in a 1:1 EC:DMC solvent at a sweep rate of 0.1 mV/s at room temperature.

Fig. 6 shows typical cyclic voltammogram (CV) curves of $LiNi_{1/3}Co_{1/3}Mn_{1/3}O_{2-z}F_z$ ($z = 0$, 0.04 and 0.08) materials between 2.5 and 4.6 V. In all curves of Fig. 6, it is noted that the appearance of only one redox couple between 2.5 and 4.6 V suggests that structural transitions from hexagonal to monoclinic structure do not exist [29]. Furthermore, no redox-reaction peaks around 3 V mean that Mn ions are not present in the +3 state [30–32]. All of the fluorine-substituted materials display similar CV to that of the $LiNi_{1/3}Co_{1/3}Mn_{1/3}O_2$, but major oxidation and reduction peaks of the substituted samples exhibit higher voltage than these of the fluorine-free material.

3. Conclusion

The layered $LiNi_{1/3}Co_{1/3}Mn_{1/3}O_{2-z}F_z$ ($z = 0$, 0.04, 0.08 and 0.12) cathode materials were successfully synthesized from oxalate precursors by a simple solvent-free self-propagating solid-state metathesis method without onerous procedures such as washing, filtering, precalcination. We investigate the effect of fluorine substitution on the structure, morphology and electrochemical properties of $LiNi_{1/3}Co_{1/3}Mn_{1/3}O_{2-z}F_z$. All samples have a phase-pure hexagonal α-$NaFeO_2$ structure with a space group of $R\bar{3}m$ and no obvious impurity phase peaks. As the fluorine content increases, the primary particle size of $LiNi_{1/3}Co_{1/3}Mn_{1/3}O_{2-z}F_z$ gradually increases. Although the fluorine-substituted materials have lower initial discharge capacities, a small amount of fluorine-substituted $LiNi_{1/3}Co_{1/3}Mn_{1/3}O_{2-z}F_z$ ($z = 0.04$ and 0.08) exhibit excellent cycling stability and rate capability compared to fluorine-free $LiNi_{1/3}Co_{1/3}Mn_{1/3}O_2$. With the help of the simple synthesis route, fluorine-substituted $LiNi_{1/3}Co_{1/3}Mn_{1/3}O_2$ cathode materials would be promising alternative of cathode materials for Lithium-ion batteries.

4. Experimental

$LiNi_{1/3}Co_{1/3}Mn_{1/3}O_{2-z}F_z$ ($z = 0$, 0.04, 0.08 and 0.12) cathode materials were synthesized by a simple self-propagating solid-state metathesis method. $Li(Ac)\cdot 2H_2O$, $Ni(Ac)_2\cdot 4H_2O$, $Co(Ac)_2\cdot 4H_2O$, $Mn(Ac)_2\cdot 4H_2O$(Ac = acetate), acetate), LiF and excess $H_2C_2O_4\cdot 2H_2O$ were used as starting materials and mixed without any solvent. The starting mixture was ball milled at 300 rpm for 3 h in a planetary mill (Puluerisett 6) with agate vessels to form an oxalate mixture as a result of the metathesis reaction between the acetate salts and $H_2C_2O_4\cdot 2H_2O$. It is apparent that the crystalline (or coordinated) water in hydrated metal salts plays an important role in the solvent-free solid-state reactions. The obtained pink colored product of ball milling was air-dried at 120 °C for 12 h and then directly calcined at 900 °C at a heating rate of 4 °C per min for 20 h in air atmosphere without precalcination procedure to obtain $LiNi_{1/3}Co_{1/3}Mn_{1/3}O_{2-z}F_z$ compounds.

The XRD patterns were recorded by a Philips 3100E diffractometer using Cu Kα radiation ($\lambda = 1.5406$ Å) to identify the crystalline phase of the as-prepared powder materials. The samples were scanned for 2θ values in the range from 10° to 80°. Unit cell parameters of $LiNi_{1/3}Co_{1/3}Mn_{1/3}O_{2-z}F_z$ materials were calculated by the least-square method using ten diffraction lines. The particle morphology of powders after calcination was observed using a field emission scanning electron microscope (FESEM, JSM-7401F, JEOL, Japan) at an accelerating voltage of 15 kV. $LiNi_{1/3}Co_{1/3}Mn_{1/3}O_{2-z}F_z$ working electrodes were prepared by slurrying 75% $LiNi_{1/3}Co_{1/3}Mn_{1/3}O_{2-z}F_z$ powder, 15% acetylene black, and 10% polyvinylidene fluoride (PVDF) in a volatile solvent, and then casting the mixture onto an aluminum foil. After vacuum drying at 120 °C for about 8 h, the electrode disks (φ14 mm) were punched and weighted. The active material loaded on the electrode disks was about 9.1 mg cm^{-2}. The $LiNi_{1/3}Co_{1/3}Mn_{1/3}O_{2-z}F_z$ working electrodes were incorporated into cells with a lithium foil counter electrode, a UP3025 separator (provided by UBE Industries, Ltd., Japan), and 1 M $LiPF_6$ electrolyte in a dimethyl carbonate (DMC) and ethylene carbonate (EC) mixed solvent of 1:1 (LP30 from EM Industries Inc.). The cells were assembled in an argon-filled glove box. Cycling performance of $LiNi_{1/3}Co_{1/3}Mn_{1/3}O_{2-z}F_z$ cathode material was evaluated using a battery test system (LAND CT2001A model, Wuhan Jinnuo Electronics Co. Ltd.) in the voltage range of 3.0–4.6V Li/Li^+ at a constant current density of 32 mA g^{-1} (0.2 C). Cyclic voltammetry (CV) was performed using a Solartron SI1287 electrochemical interface controlled by Corrware at a scanning rate 0.1 mV/s. All tests were performed at room temperature.

Acknowledgement

The authors acknowledge the partially financial support of the National Natural Science Foundation of China (No. 50236010, 20476055) and the program of New Century Excellent Talents in University of China (2004).

References

[1] T. Ohzuku, Y. Makimura, Chem. Lett. 7 (2001) 642–643.
[2] G.-H. Kim, S.-T. Myung, H.J. Bang, Jai Prakash, Y.-K. Sun, Electrochem. Solid-State Lett. 7 (2004) A477–A480.
[3] S.-H. Park, S.W. Oh, Y.-K. Sun, J. Power Sources 146 (2005) 622–625.
[4] D. Liu, Z. Wang, L. Chen, Electrochim. Acta 51 (2006) 4199–4203.
[5] Y.S. Meng, Y.W. Wu, B.J. Hwang, Y. Li, G. Ceder, J. Electrochem. Soc. 151 (2004) A1134–A1140.
[6] S.-H. Na, H.-S. Kim, S.-I. Kim, Solid State Ionics 176 (2005) 313–317.
[7] Y. Sun, Y. Xia, H. Noguchi, J. Power Sources 159 (2006) 1377–1382.
[8] G.-H. Kim, J.-H. Kim, S.-T. Myung, C.S. Yoon, Y.-K. Sun, J. Electrochem. Soc. 152 (2005) A1707–A1713.
[9] M. Kageyama, D. Li, K. Kobayakawa, Y. Sato, Y.-S. Lee, J. Power Sources 157 (2006) 494–500.
[10] C. Wu, F. Wu, L. Chen, X. Huang, Solid State Ionics 152–153 (2002) 327–334.
[11] S. Yonezawa, M. Yamasaki, M. Takashima, J. Fluorine Chem. 125 (2004) 1657–1661.
[12] G.G. Amatucci, N. Pereira, T. Zheng, J.-M. Tarascon, J. Electrochem. Soc. 148 (2001) A171–A182.
[13] X. Wu, X. Zong, Q. Yang, Z. Jin, H. Wu, J. Fluorine Chem. 107 (2001) 39–44.
[14] S.-H. Kang, K. Amine, J. Power Sources 146 (2005) 654–657.
[15] Z. Lu, D.D. MacNeil, J.R. Dahn, Electrochem. Solid-State Lett. 4 (2001) A191–A194.
[16] Y.M. Todorov, K. Numata, Electrochim. Acta 50 (2004) 495–499.
[17] M.-H. Lee, Y.-J. Kang, S.-T. Myung, Y.-K. Sun, Electrochim. Acta 50 (2004) 939–948.
[18] J. Choi, A. Manthiram, Electrochem. Solid-State Lett. 8 (2005) C102–C105.
[19] T.H. Cho, S.M. Park, M. Yoshio, T. Hirai, Y. Hideshima, J. Power Sources 142 (2005) 306–312.
[20] B.J. Hwang, Y.W. Tsai, C.H. Chen, R. Santhanam, J. Mater. Chem. 13 (2003) 1962–1968.
[21] S. Patoux, M.M. Doeff, Electrochem. Commun. 6 (2004) 767–772.
[22] A. Caballero, M. Cruz, L. Hernan, M. Melero, J. Morales, E.R. Castellon, J. Power Sources 150 (2005) 192–201.
[23] X.R. Ye, D.Z. Jia, J.Q. Yu, X.Q. Xin, Z. Xue, Adv. Mater. 11 (1999) 941–942.
[24] E.G. Gillan, R.B. Kaner, Chem. Mater. 8 (1996) 333–343.
[25] K.S. Park, M.H. Cho, S.J. Jin, K.S. Nahm, Electrochem. Solid-State Lett. 7 (2004) A239–A241.
[26] S.-W. Oh, S.-H. Park, J.-H. Kim, Y.C. Bae, Y.-K. Sun, J. Power Sources 157 (2006) 464–470.
[27] P.Y. Liao, J.G. Duh, S.R. Sheen, J. Power Sources 143 (2005) 212–218.
[28] A.R. Naghash, J.Y. Lee, Electrochim. Acta 46 (2001) 2293–2304.
[29] H. Cao, Y. Zhang, J. Zhang, B. Xia, Solid State Ionics 176 (2005) 1207–1211.
[30] S. Gopukumar, K.Y. Chung, K.B. Kim, Electrochim. Acta 49 (2004) 803–810.
[31] C. Gan, X. Hu, H. Zhan, Y. Zhou, Solid State Ionics 176 (2005) 687–692.
[32] Y.S. He, Z.F. Ma, X.Z. Liao, Y. Jiang, J. Power Sources 163 (2007) 1053–1058.